Self-Assembly of Two- and Three-Dimensional Coordination Networks with Hexamethylenetetramine and Different Silver(I) Salts

Ming-Liang Tong, Shao-Liang Zheng, and Xiao-Ming Chen*[a]

Abstract: Interesting two-dimensional networks with square or hexagonal cavities, and three-dimensional networks with different channels, have been obtained by varying the counterions, the molar ratio of metal to hmt (hmt = hexamethylenetetramine) and the pH values of the initial solutions. Among the eleven products isolated and structurally characterized, two have a metal-to-hmt molar ratio of 2:1 and are the first examples of Ag – hmt square networks, namely $[Ag_2(\mu_4\text{-hmt})(NO_2)_2]$ (**1**) and $[Ag_2(\mu_4\text{-hmt})(SO_4)(H_2O)]\cdot 4H_2O$ (**2**), two have a metal-to-hmt molar ratio of 1:1 and are 2-D networks with hexagonal cavities, namely $[Ag(\mu_3\text{-hmt})(NO_2)]$ (**3**) and $[Ag_2(\mu_3\text{-hmt})_2](S_2O_6)\cdot 2H_2O$ (**4**), and seven present the metal-to-hmt molar ratios of 3:1, 2:1, 3:2, or 4:3 and are 3-D networks of novel topologies and with different channels, namely $[Ag_2(\mu_4\text{-hmt})(\mu_4\text{-ox})]$ (**5**), $[Ag_3(\mu_4\text{-hmt})_2(H_2O)_2](SO_4)(HSO_4)\cdot 2H_2O$ (**6**), $[Ag_2(\mu_4\text{-hmt})(\mu_2\text{-}O_2CMe)](MeCO_2)\cdot 4.5H_2O$ (**7**), $[Ag_2(\mu_4\text{-hmt})(\mu_3\text{-maleate})]\cdot 5H_2O$ (**8**), $[Ag_3(\mu_4\text{-hmt})(\mu_2\text{-}O_2CPh)_3]$ (**9**), $[Ag_4(\mu_4\text{-hmt})_3(H_2O)](SO_4)(NO_3)_2\cdot 3H_2O$ (**10**), and $[Ag_{12}(\mu_4\text{-hmt})_6(\mu_3\text{-}HPO_4)(\mu_2\text{-}H_2PO_4)_3(H_2PO_4)_7(H_2O)](H_3PO_4)\cdot 10.5H_2O$ (**11**).

Keywords: coordination chemistry · hexamethylenetetramine · self-assembly · silver · supramolecular chemistry

Introduction

Pronounced interest has recently been focused on the crystal engineering of supramolecular architectures organized by coordinate covalent bonds or supramolecular contacts such as hydrogen bonding and $\pi-\pi$ interactions.[1, 2] The self-assembly of these frameworks is heavily influenced by factors such as the solvent system,[1a] the template,[3, 4] the pH value of the solution,[4] and steric requirement of the counterion;[5] the exploration of synthetic strategies and routes is therefore a long-term challenge and much work is required to extend the knowledge of the relevant structural types and establish proper synthetic strategies leading to the desired species. The use of different synthons[1a, 6, 7] is one of several strategies that could be employed in the synthesis of frameworks having large cavities or channels for possible application in separation processes and catalysis. Silver(I) is a good candidate as a simple spacer in L-M-L metallic synthons for the preparation of desired networks, and hexamethylenetetramine (hmt) as a potential tetradentate ligand seems quite suitable for self-assembly of supertetrahedral (for hmt) $[Ag_2(hmt)]$ networks with metallic synthons. However, as far as we know, no such supertetrahedral network has been isolated and characterized.[8–13]

In view of this, we tried to find a feasible route to the self-assembly of supertetrahedral $[Ag_2(hmt)]$ networks with a μ_4-hmt ligand. In a recent communication we reported the first $[Ag_2(hmt)]$ hypothetical framework with μ_4-hmt ligands and biconnected Ag^I acting as a simple spacer in L-M-L metallic synthons.[14] We report here a systematic preparation and crystal structures of eleven two- (2-D) and three-dimensional (3-D) noninterpenetrating open coordination networks self-assembled from the hmt ligand with different AgX salts (X = NO_2^-, ox^{2-} [ox = oxalate, $C_2O_4^{2-}$], SO_4^{2-}, SO_3^{2-}, $MeCO_2^-$, maleate, $PhCO_2^-$, and PO_4^{3-}): $[Ag_2(\mu_4\text{-hmt})(NO_2)_2]$ (**1**), $[Ag_2(\mu_4\text{-hmt})(SO_4)(H_2O)]\cdot 4H_2O$ (**2**), $[Ag(\mu_3\text{-hmt})(NO_2)]$ (**3**), $[Ag_2(\mu_3\text{-hmt})_2](S_2O_6)\cdot 2H_2O$ (**4**), $[Ag_2(\mu_4\text{-hmt})(\mu_4\text{-ox})]$ (**5**), $[Ag_3(\mu_4\text{-hmt})_2(H_2O)_2](SO_4)(HSO_4)\cdot 2H_2O$ (**6**), $[Ag_2(\mu_4\text{-hmt})(\mu_2\text{-}O_2CMe)](MeCO_2)\cdot 4.5H_2O$ (**7**), $[Ag_2(\mu_4\text{-hmt})(\mu_3\text{-maleate})]\cdot 5H_2O$ (**8**), $[Ag_3(\mu_4\text{-hmt})(\mu_2\text{-}O_2CPh)_3]$ (**9**), $[Ag_4(\mu_4\text{-hmt})_3(H_2O)](SO_4)(NO_3)_2\cdot 3H_2O$ (**10**), and $[Ag_{12}(\mu_4\text{-hmt})_6(\mu_3\text{-}HPO_4)(\mu_2\text{-}H_2PO_4)_3(H_2PO_4)_7(H_2O)](H_3PO_4)\cdot 10.5H_2O$ (**11**). Among these, **9** has the highest Ag:hmt molar ratio for a 3-D Ag – hmt coordination network, **1** and **2** are the first 2-D examples of Ag – hmt square networks, **3** and **4** are 2-D networks with similar skeletons and hexagonal cavities, **5** – **11** are 3-D coordination networks with novel topologies and different channels. The hmt ligands adopt the less common tetradentate mode in the construction of nine complexes, while those in **3** and **4** function in the usual tridentate mode.

[a] Prof. Dr. X.-M. Chen, Dr. M.-L. Tong, S.-L. Zheng
School of Chemistry and Chemical Engineering
Zhongshan University
Guangzhou 510275 (China)
Fax: (+86) 20-8411-2245
E-mail: cescxm@zsu.edu.cn

  0947-6539/00/0620-3729 $ 17.50+.50/0

Results and Discussion

Synthesis chemistry: All the derivatives were obtained by slow evaporation of acetonitrile–water solutions of hmt and the appropriate Ag^{I} salt in molar ratios of 1:1 or 2:1 under weak acidic or basic conditions, as shown in Scheme 1.

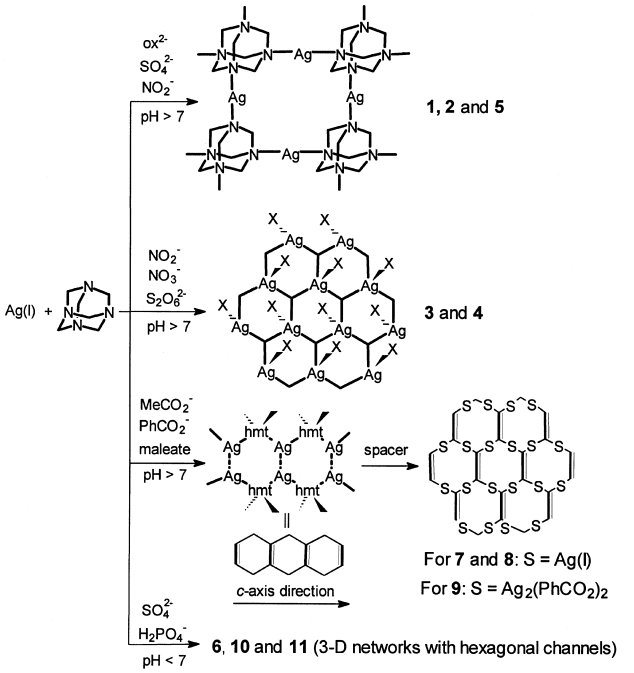

Scheme 1. Eleven different Ag–hmt networks.

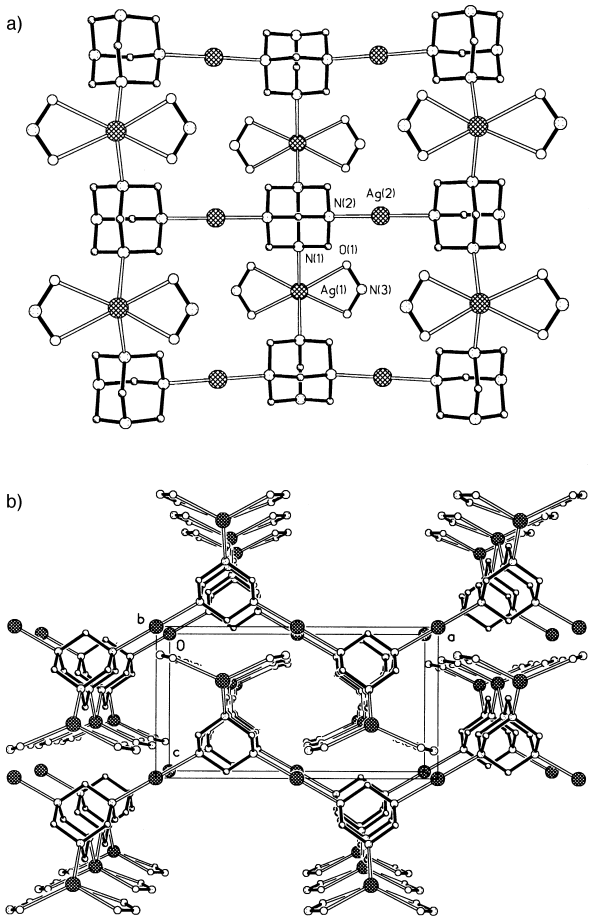

Figure 1. Perspective view of **1** showing a) the layer viewed along the *c* axis and b) the packing of the 2-D layers.

Compound **4** was obtained from self-assembly of Ag_2SO_3 and hmt. However, the counterion of the product was exchanged for $S_2O_6^{2-}$, in response to the possibility that the SO_3^{2-} counterion could be oxidized by the dioxygen molecules in air under basic conditions (relevant potentials: $\varphi^{\circ}_{OH^-/O_2} = +0.401$ V and $\varphi^{\circ}_{S_2O_6^{2-}/SO_3^{2-}} = -0.569$ V).

It is not hard to see from Scheme 1 that: 1) Participation of counterions plays an important role in self-assembly of these frameworks. Variations of the structural types of the networks were observed for different counterions. The 3-D networks were usually obtained in the presence of uncoordinated or strongly bridging counterions in the reaction systems, while the 2-D networks were easily generated in the presence of monodentate coordinating counterions in the reaction systems. 2) The pH of the solution can obviously also influence the structural type of the product, such as **2**, **6**, and **9**. 3) The $[Ag_2(hmt)]$ networks, which have been theoretically postulated but not isolated,[11] can be easily obtained by our synthetical routes in a polar acetonitrile–water solvent.

Crystal structures

2-D square nets: Nets **1** and **2** are made up of infinite, undulating neutral 2-D layers of square units. As illustrated in Figure 1a, each square unit of **1** is organized from four Ag^{I} atoms in two geometries and four hmt ligands each at the midpoints of sides and corners, in which the Ag(1) atom, located at a two-fold crystallographic axis, is in a greatly distorted octahedron coordinated by two nitrogen atoms from different hmt ligands [Ag(1)–N 2.479(3) Å, N-Ag(1)-N 101.79(15)°] and four oxygen atoms from two chelated NO_2^- groups [Ag(1)–O 2.499(3) Å, O-Ag(1)-O 49.65(12)°], while the Ag(2) atom is in a perfectly linear geometry ligated by two nitrogen atoms from two hmt ligands [Ag(2)–N 2.294(3) Å, N-Ag-N 180°].

Adjacent layers are separated by a distance of 6.945 Å and are intercalated into each other by the lateral Y-shaped $Ag(NO_2)_2$ fragments of one layer inserting into the U-shaped cavities of two adjacent layers, where weak interlayer Ag···O contacts (2.865 Å) between the biconnected Ag^{I} atoms and oxygen atoms of the NO_2^- group result in a 3-D molecular network (Figure 1b).

The structure of **2** is also made up of infinite, deeply undulating neutral 2-D layers of square units similar to those of **1** together with lattice water molecules.[14] As depicted in Figure 2, each square unit is organized from four Ag^{I} atoms in two geometries and four hmt molecules each at the midpoints of sides and corners; the Ag(2) atom is in a distorted trigonal geometry coordinated by two nitrogen atoms from different hmt ligands and one aquo ligand [Ag(2)–N 2.311(4) and 2.347(4), Ag(2)–O 2.303(4) Å; N-Ag(2)-N (or O) 115.10(14)–127.80(15)°), while the Ag(1) atom is in a T-shaped geometry ligated by two nitrogen atoms from two

0947-6539/00/0620-3730 $ 17.50+.50/0 *Chem. Eur. J.* **2000**, *6*, No. 20

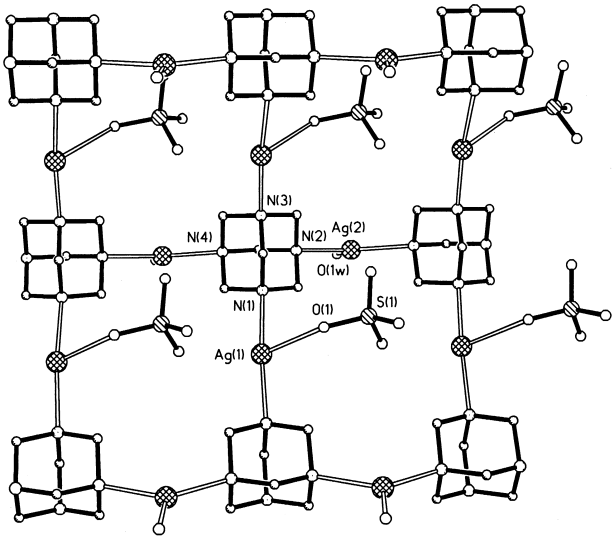

Figure 2. Perspective view showing a layer in **2**.

hmt ligands and one monodentate SO_4^{2-} anion [Ag(1)–N 2.279(4) and 2.292(4), Ag(1)–O 2.571(5) Å; N-Ag(1)-N 172.81(15), N-Ag(1)-O 88.44(16) and 92.44(15)°].

In contrast to that of **1**, adjacent layers of **2** are connected by interlayer hydrogen bonds between the aquo ligand and SO_4^{2-} anion with the O(1w)···O(SO_4) distance of 2.681–2.691 Å, resulting in a 3-D molecular network having irregular pentagonal channels. The lattice water molecules are clathrated in these channels.

To our knowledge, hmt usually acts in a μ_3-bridged mode in construction of most of the 2-D Ag–hmt nets[8, 11, 12] and no square-grid structural motif in 2-D Ag–hmt networks was known before our work; the square 2-D nets in **1** and **2** are, therefore, a new structural motif and the first examples constructed from μ_4-hmt in 2-D Ag–hmt nets.

2-D hexagonal nets: The networks of **3** and **4** are made up of infinite wavy 2-D layers of hexagonal units in the boat-type conformation, similar to those in [Ag(hmt)]X (X = NO_3^-, ClO_4^-, and SbF_6^-).[8, 11, 12] As illustrated in Figure 3a, each hexagonal unit in **3** is organized from three Ag^I atoms and three hmt ligands, each representing a corner. The Ag^I atom occupies a greatly distorted tetrahedral geometry, coordinated by three nitrogen atoms from different hmt ligands [Ag(1)–N 2.399(5)–2.438(4) Å, N-Ag(1)-N 110.18(10)–115.13(17)°] and one oxygen atom from a monodentate NO_2^- ion [Ag(1)–O 2.444(10) Å, N-Ag(1)-O 93.8(2)–112.74(12)°]. These NO_2^- ions are alternately oriented above and below the hexagonal layer.

Adjacent layers are separated by 6.475 Å and have no significant interlayer connection (Figure 3b), being similar to those in [Ag(hmt)]X (X = NO_3^-,[8] ClO_4^-,[11] and SbF_6^-[12]), but different from those in **1** and **2**.

Each hexagonal unit in **4** is also organized from three Ag^I ions and three hmt molecules making up the corners, as in **3**. But the Ag^I atom is in a slightly distorted trigonal geometry, coordinated by three nitrogen atoms from different hmt ligands [Ag(1)–N 2.336(4)–2.354(4) Å, N-Ag(1)-N 117.71(13)–123.39(13)°], as illustrated in Figure 4a.

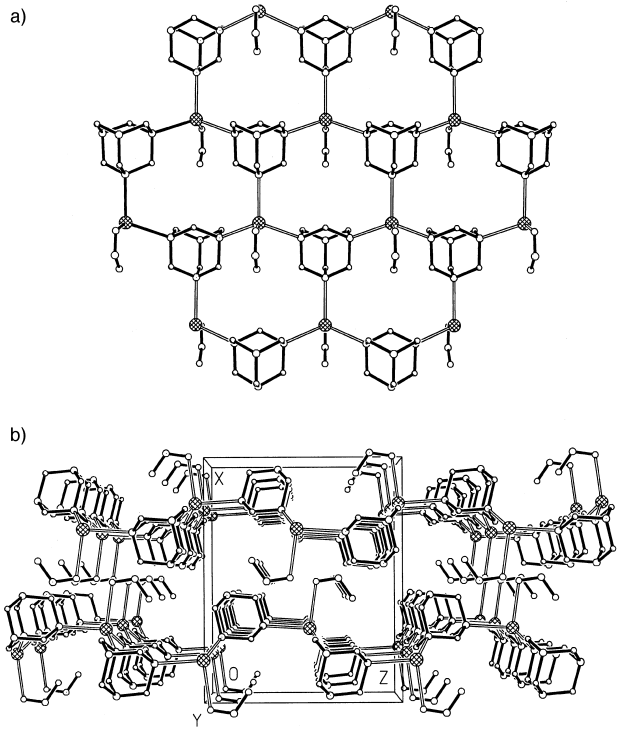

Figure 3. Perspective view showing a) a layer and b) the packing of the 2-D layers in **3**.

The $S_2O_6^{2-}$ anions are located in orderly fashion between the 2-D layers with weak Ag···O(S_2O_6) bonds [2.728(5) Å], thus acting as pillars between the 2-D layers to produce 1-D channels in the *a* axis in the solid, as shown in Figure 4b.

3-D coordination networks: The structure of **5** consists of 2-D [Ag_2(hmt)] square nets similar to those of **1** and **2**, which are further connected by μ_4-ox^{2-} bridges to form a 3-D coordination network. As in **1** and **2**, each square unit of the 2-D net is organized of four Ag^I atoms in two geometries and four hmt molecules, one each at the midpoints of sides and corners; the Ag(1) ion occupies a distorted octahedral geometry, coordinated by two nitrogen atoms from different hmt ligands and four oxygen atoms from two ox^{2-} ligands [Ag(1)–N 2.500(5), Ag(1)–O 2.492(6) and 2.545(6) Å], while the Ag(2) atom is in a distorted tetrahedral geometry ligated by two nitrogen atoms from two hmt ligands [Ag(2)–N 2.413(5) Å] and two oxygen atoms from different ox^{2-} ligands belonging to the adjacent upper or lower layer [Ag(2)–O 2.486(6) Å]. Therefore, the 2-D square layers are interlinked by μ_4-ox^{2-} bridges into a 3-D network (Figures 5a and b). It has been documented that the ox^{2-} ligand can act in μ_6-bridge mode ligating Ag^I atoms;[15a,b] the μ_4 mode present here (Figure 5c) has not been reported elsewhere, although μ_2, μ_3, μ_4, μ_5, μ_6, and μ_8 modes have been observed for other metal atoms.[15c–j]

The structure of **6** consists of an open 3-D cationic network formed by the same hexagonal [Ag(hmt)] layers (Figure 6a) as those in **3** and **4**, joined by biconnected Ag^I atoms, which coordinate to the fourth nitrogen atoms (free in **3** and **4**) of the hmt ligands, as shown in Figure 6b. The Ag–N bond lengths [2.249(5) Å] for these spacers are shorter than those [2.312(5)–2.367(3) Å] in [Ag(hmt)] layers, but slightly longer

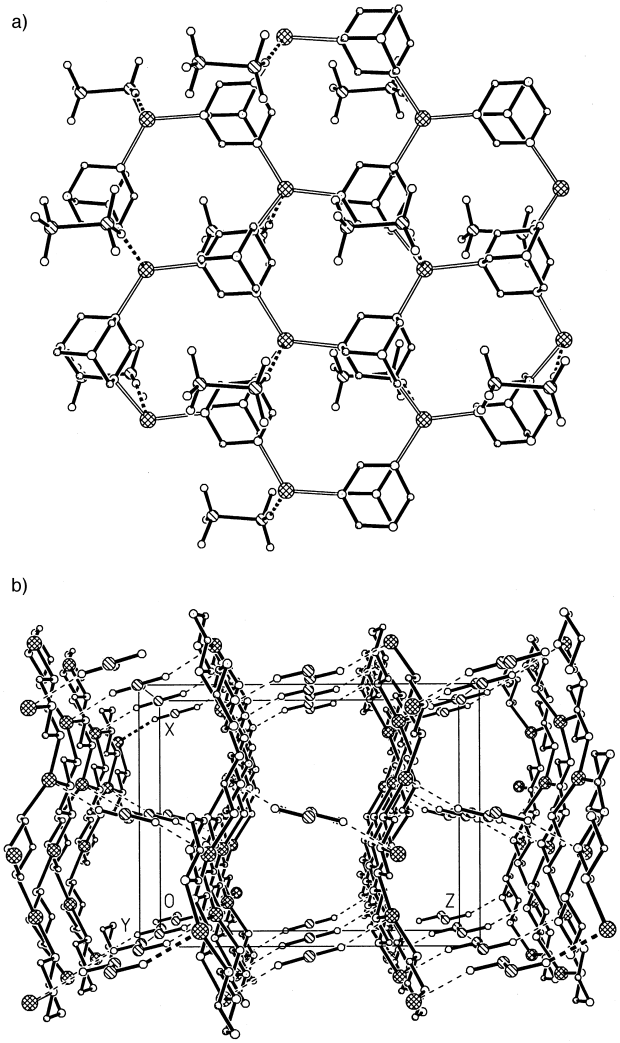

Figure 4. Perspective view showing a) a layer and b) the packing of the 2-D layers in **4**. The uncoordinated nitrogen atoms and their adjacent carbon atoms of the hmt ligands in (b) have been omitted for clarity.

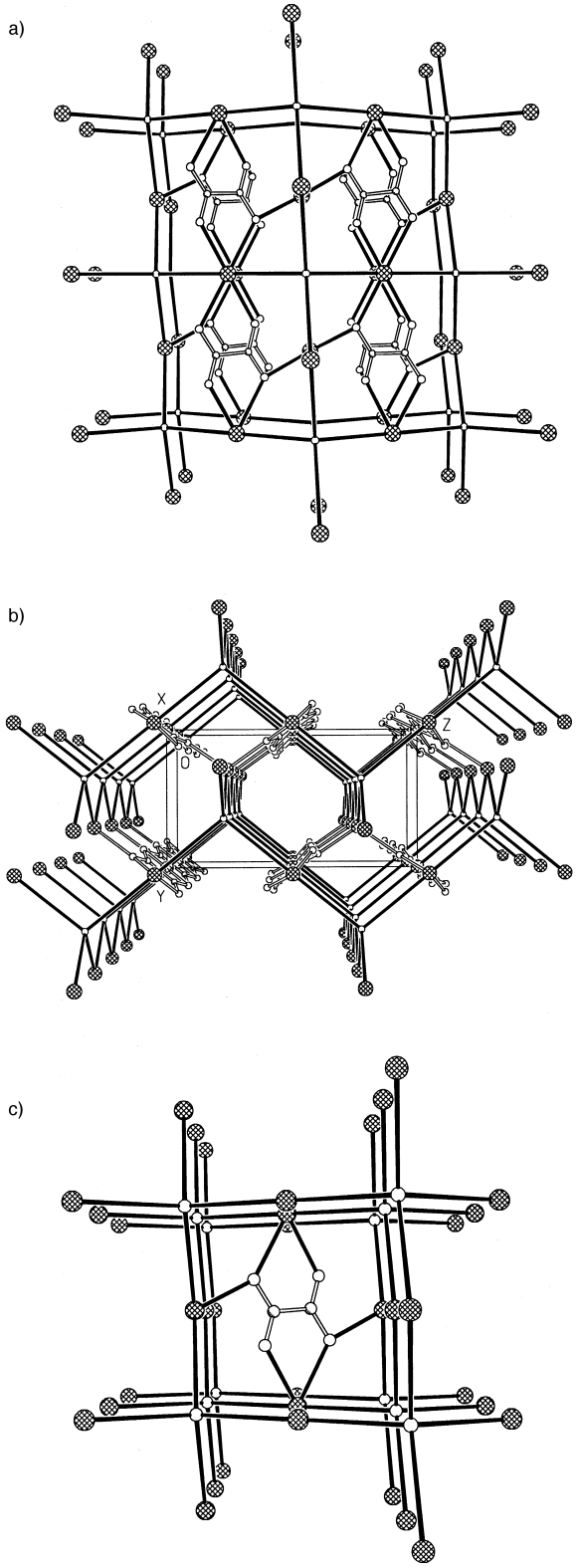

Figure 5. a) Perspective view of **5** showing the 3-D network viewed along the *b* axis and b) the *a* axis, and c) the coordination mode of the ox^{2-} group. Small open balls represent centers of mass of the hmt ligands.

than those [2.223(5) Å] found in a similar 3-D network, $[Ag_3(hmt)_2](ClO_4)_3 \cdot 2H_2O$.[13] The SO_4^{2-}, HSO_4^-, and lattice water molecules are clathrated in the hexagonal channels.

From the topological point of view, the 3-D network of **6** is a (3,4)-connected net, comprising triconnected (silver atoms of the layers) and tetraconnected (hmt molecules) centers in the ratio 1:1, similar to those of $[Ag_3(hmt)_2](ClO_4)_3 \cdot 2H_2O$[11] and $[Ag_{11}(hmt)_6](PF_6)_3 \cdot 14H_2O$.[12]

The structure of **7** is an open 3-D cationic honeycomb network with hexagonal channels, acetate counterions, and lattice water molecules.[14] As shown in Scheme 1, the dimeric $Ag_2(MeCO_2)_2$ fragments are bridged by hmt ligands, each using two nitrogen atoms, to create an infinite chain with hexagonal cavities along the *c* direction [Ag–N 2.240(4) and 2.405(4), Ag–O 2.366(4) and 2.391(4) Å]. These chains are further joined by simple Ag^I spacers through the two remaining nitrogen atoms of the hmt ligands [Ag–N 2.238(5) and 2.255(5) Å; N-Ag-N 178.08(15)°] into a 3-D noninterpenetrating open network having hexagonal channels along the *c* axis (Figure 7a). The uncoordinated acetate ions and lattice water molecules are clathrated in the channels and hydrogen-bonded to each other and to the carboxylate groups of the host network.

The topology in **7** is, to the best of our knowledge, unprecedented. The hexagonal subunits viewed along the *c*

  0947-6539/00/0620-3732 $ 17.50+.50/0 *Chem. Eur. J.* **2000**, *6*, No. 20

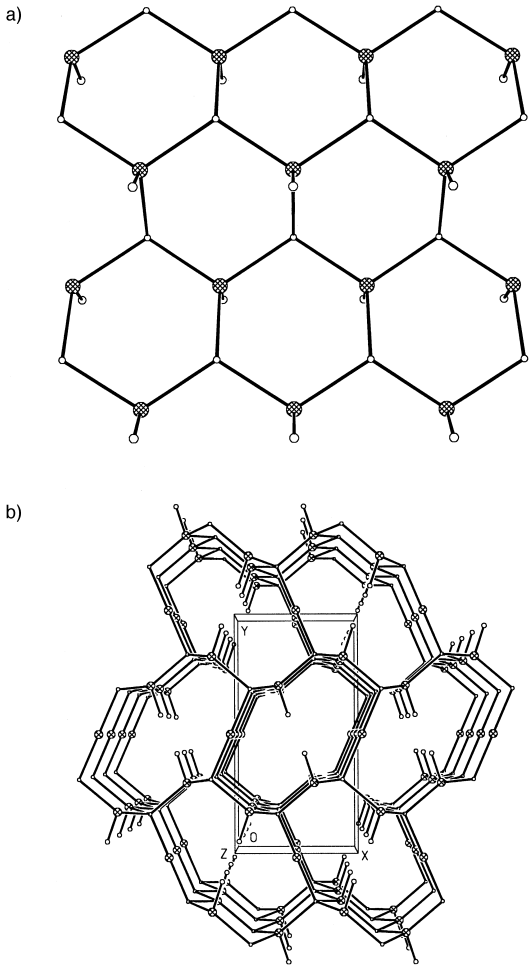

Figure 6. Perspective view of **6** showing a) the 2-D layer and b) the 3-D network along the *c* axis. Small open balls represent centers of mass of the hmt ligands.

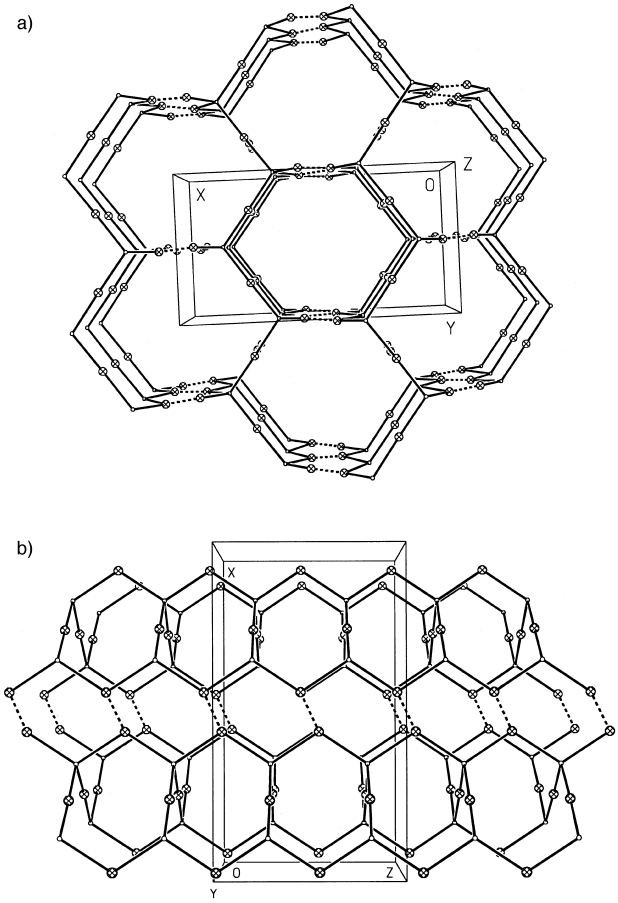

Figure 7. Perspective view showing the 3-D network in **7** along a) the *c* axis and b) the *b* axis. The μ_2-O_2CMe bridges are omitted for clarity. Small open balls represent centers of mass of the hmt ligands.

axis are all equivalent (Figure 7a), and involve four Ag^I atoms, two $Ag_2(O_2CMe)_2$ fragments, and six hmt ligands, while the hexagonal subunits viewed along the *b* axis are nonequivalent and can be classified into two categories (Figure 7b); one involves two $Ag_2(O_2CMe)_2$ fragments and two hmt ligands, another involves four Ag^I atoms and four hmt ligands. These features are in contrast to those of the reported three-dimensional networks, a triconnected 3-D enantiomorphic interpenetrating network in $[Ag(hmt)]PF_6 \cdot H_2O$,[10] two (3,4)-connected nets in $[Ag_3(hmt)_2](ClO_4)_3 \cdot 2H_2O$[11] and $[Ag_{11}(hmt)_6](PF_6)_{11} \cdot 14H_2O$,[12] and a triconnected 3-D net in $[Ag_4(hmt)_3(H_2O)](PF_6)_4 \cdot 3EtOH$.[13] The hexagonal units of the 3-D network of **7** are all equivalent and involve four Ag^I atoms, two $Ag_2(\mu_2\text{-}O_2CMe)_2$ fragments, and six hmt ligands. In the $Ag_2(\mu_2\text{-}O_2CMe)_2$ fragments, the Ag^I atoms are joined by two unusual noncoplanar skew–skew μ_2-carboxylate bridges[16] with an Ag···Ag distance of 2.9144(8) Å, indicating a relatively strong Ag···Ag interaction;[17] each Ag^I atom is further ligated by two nitrogen atoms from two different hmt ligands, completing a distorted tetrahedron.

The structure of **8** is similar to that of **7** and also consists of an open 3-D neutral honeycomb network with hexagonal subunits (Figure 8a) and lattice water molecules. The dimeric $Ag_2(maleate)_2$ fragments, each formed by a pair of silver(I) atoms bridged by two μ_2-carboxylate ends from two maleate ligands, are joined by a bridge of the hmt ligands, each using two nitrogen atoms, to form an infinite chain along the *c* axis [Ag···Ag 2.8154(15), Ag–N 2.238(5)–2.304(4), and Ag–O 2.475(4)–2.530(5) Å]. These chains are further joined by the simple Ag^I spacers through the two remaining nitrogen atoms of the hmt ligand [Ag–N 2.269(4) and 2.287(4) Å; N-Ag-N 162.48(16)°] into a 3-D noninterpenetrating open network having hexagonal channels along the *c* or *b* axis (Figure 8b). Another carboxylate end of the maleate ligand ligates in monodentate fashion to an adjacent Ag^I atom (Ag–O 2.534(5) Å). Although the hexagonal channels are mainly occupied by the alkene units of the maleate groups, a large number of lattice water molecules are located in them, hydrogen-bonded to one other and to the carboxylate groups of the host network [O···O 2.676(7)–2.947(10) Å].

It should be noted that, neglecting the Ag–maleate coordination, the topology of **8** is the same as that of **7**.

Crystals of **9** are made up of a neutral 3-D honeycomb coordination network with hexagonal subunits (Figure 9a). As shown in Scheme 1, the dimeric $Ag_2(PhCO_2)_2$ fragments are bridged by hmt ligands, each using two nitrogen atoms, to form an infinite chain along the *a* axis, which is similar to that in **7** and **8**.[14] These chains are further joined by the

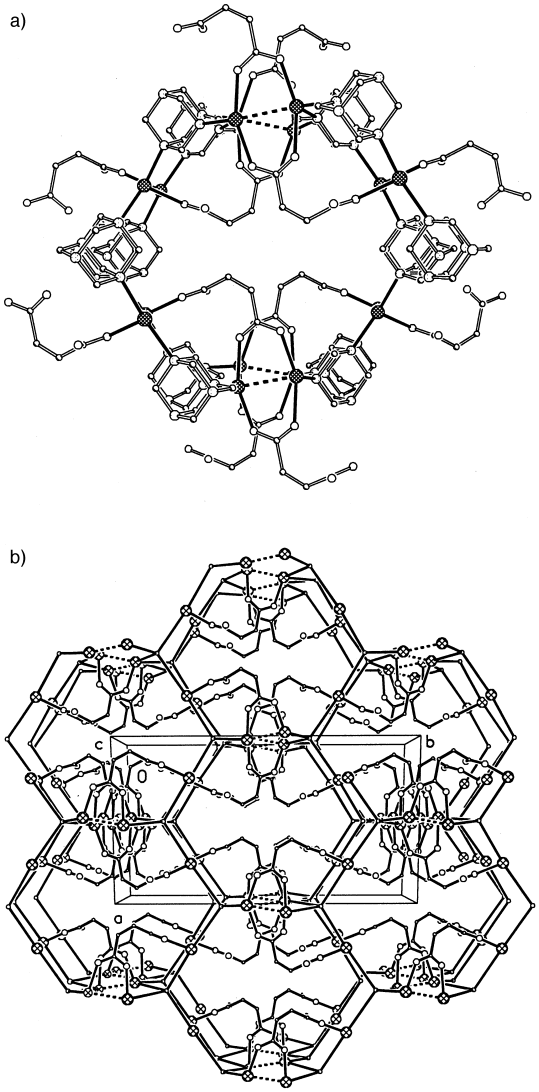

Figure 8. Perspective view of **8** showing a) the hexagonal ring and b) the 3-D network along the *c* axis. Small open balls represent centers of mass of the hmt ligands.

biconnected $Ag_2(PhCO_2)_2$ fragments through the two remaining nitrogen atoms of the hmt ligands into a novel 3-D honeycomb network. It should be noted that the biconnected $Ag_2(PhCO_2)_2$ fragments present here act as a longer spacer than those in **7** and **8**, an unprecedented observation.

The $Ag_2(\mu_2\text{-}O_2CPh)_2$ fragments can be classified into three types. As shown in Figure 9a, the first type of Ag^I atom is joined by two unusual noncoplanar skew–skew carboxylate bridges[16] with an Ag–Ag distance of 2.8567(15) Å, indicating a relatively strong Ag···Ag interaction;[17] each Ag^I atom is further ligated by two nitrogen atoms from two different hmt ligands, completing a tetrahedral coordination geometry [Ag(1)–O 2.269(7) and 2.253(7), Ag(1)–N 2.416(7) and 2.441(6) Å], while the second or third type of Ag^I atom is ligated by two oxygen atoms from the skew–skew or coplanar carboxylate bridges [Ag···Ag distance of 2.8186(20) and 2.7460(18) Å] and one nitrogen atom from one hmt ligand, resulting in a distorted T-shaped coordination geometry [Ag(2)–O 2.223(6) and 2.231(6), Ag(2)–N 2.415(7); Ag(3)–O 2.159(6) and 2.204(7), Ag(3)–N 2.435(7) Å].

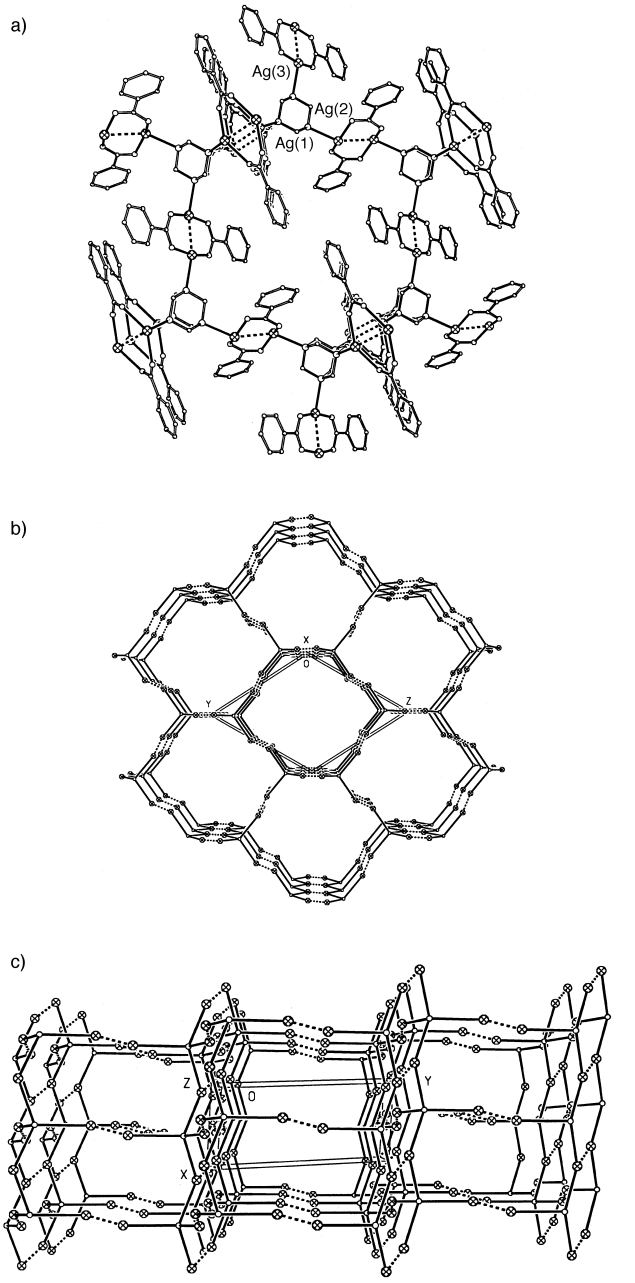

Figure 9. Perspective view of **9** showing a) the hexagonal ring, b) the 3-D network seen along the *a* axis and c) along the *b* axis. The μ_2-O_2CPh bridges are omitted for clarity and small open balls represent centers of mass of the hmt ligands in (b) and (c).

It is noteworthy that **9** is the 3-D Ag–hmt coordination network with the highest molar ratio of Ag to hmt, and the topology of **9** is, to the best of our knowledge, unprecedented. In **9**, each hexagonal unit viewed along the *a* axis is equivalent, and involves six $Ag_2(O_2CPh)_2$ fragments and six hmt ligands (Figure 9b), while the rectangular unit viewed along the *b* or *c* axis involves four hmt ligands and four $Ag_2(O_2CPh)_2$ fragments in two types. The long side is hmt-$Ag_2(O_2CPh)_2$-hmt, the short one is hmt-Ag-hmt (Figure 9c). These features are different from those of **7** and **8**. It has been reported that the largest ring in observed Ag–hmt networks is composed of six biconnected Ag^I atoms and six hmt ligands, so the hexagonal

  0947-6539/00/0620-3734 $ 17.50+.50/0 *Chem. Eur. J.* **2000**, *6*, No. 20

ring in **9** becomes the largest one so far in Ag–hmt networks, being composed of twelve Ag^I atoms and six hmt ligands (Figure 9a).

The structure of **10** is a novel open 3-D cationic network with two types of channels, as depicted in Figure 10. Four crystallographically independent Ag^I atoms have three types

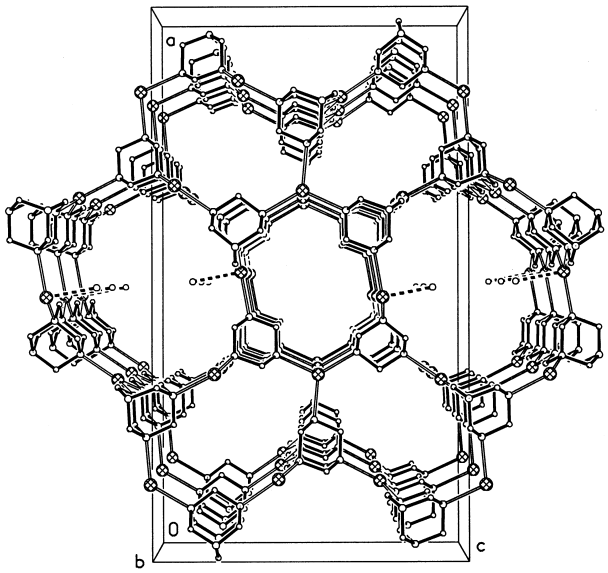

Figure 10. Perspective view of **10** showing the 3-D network along the *b* axis.

of coordination geometry. The setting of the first type of Ag(1) atoms has a distorted tetrahedral geometry due to coordination by three nitrogen atoms from three hmt ligands [Ag–N 2.384(7)–2.385(5) Å; N-Ag-N 117.8(2)–120.98(11)°] and one oxygen atom from an aquo ligand [Ag–O 2.558(9) Å; N-Ag-O 89.1(3)–93.19(17)°]. Each of the second type of Ag^I atoms occupies a slightly distorted triangular geometry and is coordinated by three nitrogen atoms from three hmt ligands [Ag–N 2.343(7)–2.389(5) Å; N-Ag-N 117.6(2)–121.20(12)°]. Each of the third type of Ag^I atom is in a Y-shaped geometry and coordinated by three nitrogen atoms from three hmt ligands [Ag–N 2.350(7)–2.389(5) Å; N-Ag-N 109.5(2) and 125.3(2)°].

It is noteworthy that, from the topological point of view, the 3-D network of **10** is also a (3,4)-connected net, composed of triconnected (silver atoms of the layers) and tetraconnected (hmt molecules) centers. But the topological type is unprecedented. The large hexagonal unit of the 3-D network of **10** involves six Ag^I atoms and six hmt ligands, while the small one involves four Ag^I atoms and four hmt ligands; each large hexagonal unit is enclosed by six small hexagonal ones, and each small one is enclosed by two large ones and four small ones. These features are different from those of the triconnected 3-D net in $[Ag_4(hmt)_3(H_2O)](PF_6)_4 \cdot 3EtOH$,[13] which has a similar formula to **10**, but contains silver(I) atoms and hmt ligands with different coordination geometry and coordination modes, and therefore a different network skeleton; they are also different from those in **6**–**9** and the reported 3-D Ag–hmt networks, a triconnected 3-D enantiomorphic interpenetrating network in $[Ag(hmt)]PF_6 \cdot H_2O$,[10] and two (3,4)-connected 3-D nets in $[Ag_3(hmt)_2](ClO_4)_3 \cdot 2H_2O$[11] and $[Ag_{11}(hmt)_6](PF_6)_{11} \cdot 14H_2O$.[12]

The structure of **11** consists of an open neutral 3-D network with hexagonal channels, neutral H_3PO_4 molecules, and lattice water molecules. As shown in Figure 11a, twelve crystallographically independent Ag^I atoms have four types of coordination geometry. Ag(1), Ag(4), Ag(5), Ag(6), and Ag(11) atoms are in distorted tetrahedral geometry; each is coordinated by two nitrogen atoms from two hmt ligands and two oxygen atoms from two $H_2PO_4^-$ ions, or one $H_2PO_4^-$ and one HPO_4^{2-} ion, or one $H_2PO_4^-$ ion and an aquo ligand [Ag–N 2.297(10)–2.403(11), Ag–O 2.259(12)–2.548(13) Å]. Ag(2) and Ag(9) atoms occupy a T-shaped geometry and are each coordinated by two nitrogen atoms from two hmt ligands and one oxygen atom from one $H_2PO_4^-$ group [Ag–N 2.224(12)–2.316(13), Ag(2)–O 2.574(11)–2.587(13) Å]. Ag(3), Ag(7), and Ag(10) atoms are in distorted triangular geometry and are each coordinated by two nitrogen atoms from two hmt ligands and one oxygen atom from one $H_2PO_4^-$

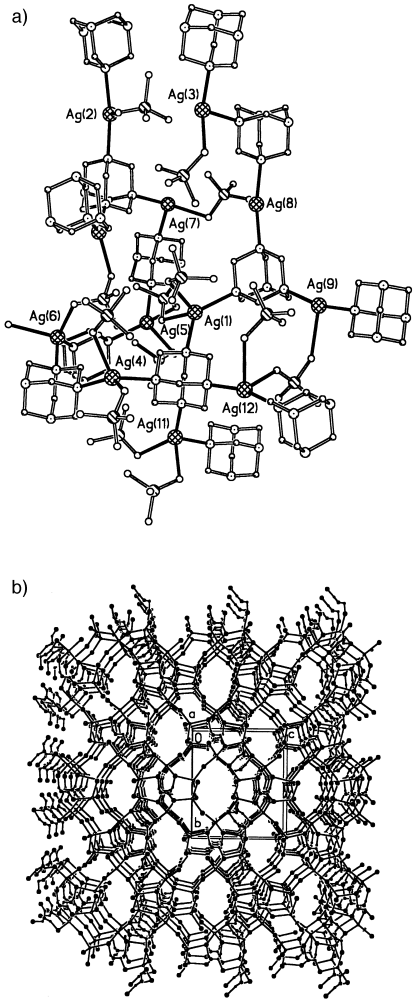

Figure 11. a) Coordination environments of the metal atoms in **11;** b) perspective view showing the 3-D network in **11** along the *a* axis. Small open balls represent centers of mass of the hmt ligands. The monodentate $H_2PO_4^-$ and the uncoordinated oxygen atoms of the bridging $H_2PO_4^-$ or HPO_4^{2-} groups are omitted for clarity.

ion [Ag(10)–N 2.295(12)–2.394(14), Ag(3)–O 2.281(12)–2.413(18) Å], the Ag(12) atom is in an uncommon square-planar geometry[18] and is coordinated by two nitrogen atoms from two hmt ligands and two oxygen atoms from two $H_2PO_4^-$ ions [average Ag(12)–N 2.222(12), Ag(12)–O 2.514(12) Å].

Among the twelve crystallographically independent HPO_4^{2-}, $H_2PO_4^-$ groups and H_3PO_4 molecules, one acts as a μ_3 bridge, three as μ_2 bridges, and seven in monodentate mode in coordination to the Ag^I atoms, and the neutral H_3PO_4 molecule is hydrogen-bonded to the lattice water molecules and the coordinated HPO_4^{2-} or $H_2PO_4^-$ groups.

Such coordination geometries and bridging modes interact in complex form to generate the 3-D network of hexagonal channels (Figure 11b). It is noteworthy that the channels in **11** are asymmetric, a useful property in microporous solids for selective molecular adsorption, ion exchange, and heterogeneous catalysis.[19]

Thermogravimetric analysis: In order to examine the thermal stability of the porous networks, we carried out thermogravimetric (TG) analyses and measurements of the XRPD patterns for some structures. Samples of **2**, **4**, **7**, **8**, **9**, and **10** were chosen to be heated to 600 °C in N_2. The TGA curve for **2** shows that the first weight loss of 13.1% between 76 and 100 °C corresponds to the loss of the included water molecules (calculated: 13.3%), and the second weight loss of 3.2% between 100 and 156 °C corresponds to the loss of coordinated water molecules (calculated: 3.3%). Decomposition of **2** began above 205 °C. The TGA curve for **4** shows that the first weight loss of 2.5% between 50 and 98 °C corresponds to the loss of one included water molecule (calculated: 2.6%), and the second weight loss of 2.4% corresponds to the loss of the second included water molecule between 98 and 177 °C (calculated: 2.6%). Decomposition of **4** began above 240 °C. The TGA curve for **7** shows that the weight loss of 14.3% between 70 and 120 °C corresponds to the loss of the included water molecules (calculated: 14.6%). Decomposition of **7** began above 208 °C. The TGA curve for **8** shows that the weight loss of 15.6% between 50 and 157 °C corresponds to the loss of five included water molecules (calculated: 16.1%). Decomposition of **8** began above 220 °C. The TGA curve for **10** shows that the weight loss of 6.6% between 100 and 180 °C corresponds to the loss of the three included water molecules and one aquo ligand (calculated: 6.3%). This fact indicates that the aquo ligand is weakly coordinated, in accordance with the relatively long Ag–O bond revealed in its crystal structure. Decomposition of **10** began above 220 °C. The TGA curves show that no chemical decomposition occurred up to 200 °C and 220 °C for **4** and **9**, respectively. The X-ray powder diffraction patterns of these samples are more or less different from those of the original solids and a slight shift and broadening of the diffraction lines was observed along with the emergence of new small diffraction lines; these phenomena indicate alteration of the crystal structure topologies or local distortions within the structures, which are commonly observed in zeolites and molecular sieves,[20] and may be attributed to distortions in the pore structures which often lower the overall symmetry of the structures slightly when the solvate molecules are driven from the pores.[21] Even so, the fact that no chemical decomposition was observed up to 200–240 °C for the Ag–hmt networks present here and documented elsewhere[10, 11] suggests that they may, in a sense, be related to the porous materials.

Conclusion

Interesting two-dimensional networks, with square or hexagonal cavities, and three-dimensional networks of novel topologies have been obtained from the self-assembly of the rigid μ_3- or μ_4-hmt ligand and different silver salts depending on the counterions, the molar ratio of metal to hmt, and the pH values of the solutions. Variations in the structural motifs of the networks have been observed with increasing coordination ability of the counterions. The 3-D networks were usually obtained in the presence of uncoordinated or strongly bridging counterions in the reaction systems, while the 2-D networks were easily generated in the presence of monodentate coordinating counterions in the reaction systems. Out of the eleven products isolated and characterized, two have a metal-to-hmt molar ratio of 2:1 and contain 2-D square structural motifs, namely $[Ag_2(\mu_4\text{-hmt})(NO_2)_2]$ (**1**) and $[Ag_2(\mu_4\text{-hmt})(SO_4)(H_2O)]\cdot 4H_2O$ (**2**), two have a metal-to-hmt molar ratio of 1:1 and contain 2-D hexagonal networks, $[Ag(\mu_3\text{-hmt})(NO_2)]$ (**3**) and $[Ag_2(\mu_3\text{-hmt})_2](S_2O_6)\cdot 2H_2O$ (**4**), seven present 3-D networks with novel topologies and channels of different sizes, specifically $[Ag_2(\mu_4\text{-hmt})(\mu_4\text{-ox})]$ (**5**), $[Ag_3(\mu_4\text{-hmt})_2(H_2O)_2](SO_4)(HSO_4)\cdot 2H_2O$ (**6**), $[Ag_2(\mu_4\text{-hmt})(\mu_2\text{-}O_2CMe)](MeCO_2)\cdot 4.5H_2O$ (**7**), $[Ag_2(\mu_4\text{-hmt})(\mu_3\text{-maleate})]\cdot 5H_2O$ (**8**), $[Ag_3(\mu_4\text{-hmt})(\mu_2\text{-}O_2CPh)_3]$ (**9**), $[Ag_4(\mu_4\text{-hmt})_3(H_2O)](SO_4)(NO_3)_2\cdot 3H_2O$ (**10**) and $[Ag_{12}(\mu_4\text{-hmt})_6(\mu_3\text{-}HPO_4)(\mu_2\text{-}H_2PO_4)_3(H_2PO_4)_7(H_2O)](H_3PO_4)\cdot 10.5H_2O$ (**11**).

Although hmt rarely acts in tetradentate coordination mode, our present work suggests effective routes to constructing $[Ag_2(hmt)]$ frameworks with μ_4-hmt ligands and metallic spacers. Moreover, the longer $Ag_2(\mu_2\text{-}O_2CPh)_2$ entities have been successfully used as a simple spacer to construct a novel 3-D noninterpenetrating honeycomb network with the highest Ag^I:hmt molar ratio to date. The isolation of the title complexes and previous work also demonstrate that participation of counterions plays a vital role in self-assembly of these frameworks.

Experimental Section

Materials: The $AgNO_2$, $Ag_2(ox)$ and Ag_2SO_3 salts were prepared by the reaction of $AgNO_3$ and the appropriate sodium salts, Ag_3PO_4 was prepared by the reaction of Ag_2O and dilute H_3PO_4 solution, $Ag_2(maleate)_2$ and $Ag_2(PhCO_2)_2$ were prepared according to the literature method.[22] Other reagents and solvents employed were commercially available and used as received without further purification. The C, H, N microanalyses were carried out with a Perkin–Elmer 240 elemental analyzer. The FT-IR spectra were recorded from KBr pellets in range 4000–400 cm^{-1} on a Nicolet 5DX spectrometer. Thermogravimetric data were collected on a Perkin–Elmer TGS-2 analyzer in flowing nitrogen at a heating rate of 10 °C min^{-1}.

Synthesis of the polymers: All the compounds were prepared by treating the silver salts ($AgNO_2$, Ag_2SO_4, Ag_2SO_3, $Ag_2(ox)$, $Ag_2(O_2CMe)_2$, $Ag_2(maleate)_2$, $Ag_2(PhCO_2)_2$, and Ag_3PO_4) dissolved in MeCN/H_2O mixed solvents with MeCN solution of the hmt ligand in molar ratios of 1:1 or 1:2 at 50–60 °C.

0947-6539/00/0620-3736 $ 17.50+.50/0 *Chem. Eur. J.* **2000**, *6*, No. 20

Synthesis of $[Ag_2(\mu_4\text{-hmt})(NO_2)_2]$ (1): An aqueous solution (5 mL) of hmt (0.140 g, 1.0 mmol) was added dropwise to a stirred MeCN/H_2O solution (5 mL) of $AgNO_2$ (0.308 g, 2.0 mmol) at 50 °C for 15 min. The resulting colorless solution was allowed to stand in air at room temperature for two weeks, yielding colorless crystals in good yield (78 %). Anal. calcd for $C_6H_{12}Ag_2N_6O_4$ **1**: C 16.09, H 2.70, N 18.76 %; found: C 15.92, H 2.56, N 18.66 %; IR (KBr, cm^{-1}): $\tilde{\nu}$ = 3451 m br, 2981 w, 2852 m, 2876 w, 1578 m, 1460 s, 1377 m, 1328 m, 1267 s, 1238 vs, 1006 vs, 928 m, 806 s, 687 s, 666 m, 512 m.

Synthesis of $[Ag_2(\mu_4\text{-hmt})(SO_4)(H_2O)]\cdot 4H_2O$ (2): The procedure was the same as that for **1**, yield ca. 75 %. Anal. calcd for $C_6H_{22}Ag_2N_4O_9S$ **2**: C 13.29, H 4.09, N 10.34 %; found: C 13.16, H 4.02, N 10.22 %; IR (KBr, cm^{-1}): $\tilde{\nu}$ = 3437 m br, 3395 m, 2966 w, 2938 m, 2868 m, 1651 m, 1560 m, 1454 m, 1384 m, 1370 m, 1229 s, 1117 vs, 1004 vs, 835 w, 814 s, 688 m, 617 s, 512 m.

Synthesis of $[Ag(\mu_3\text{-hmt})(NO_2)]$ (3): The procedure was the same as that for **1** except that the molar ratio of Ag:hmt was 1:1, yield ca. 85 %. Anal. calcd for $C_6H_{12}AgN_5O_2$ **3**: C 24.51, H 4.11, N 23.82 %; found: C 24.38, H 4.06, N 23.76 %; IR (KBr, cm^{-1}): $\tilde{\nu}$ = 3458 m, 2950 m, 2874 m, 1630 w, 1459 m, 1371 m, 1269 vs, 1239 vs, 1006 vs, 812 s, 687 m, 512 m.

Synthesis of $[Ag_2(\mu_3\text{-hmt})_2](S_2O_6)\cdot 2H_2O$ (4): The procedure was the same as that for **1** except that the molar ratio of Ag:hmt was 1:1, yield ca. 75 %. Anal. calcd for $C_{12}H_{28}Ag_2N_8O_8S_2$ **4**: C 20.82, H 4.08, N 16.19 %; found: C 20.68, H 4.02, N 16.11 %; IR (KBr, cm^{-1}): $\tilde{\nu}$ = 3465 m, 2954 w, 2886 w, 1636 w, 1463 m, 1385 w, 1226 vs, 1008 vs, 988 vs, 927 w, 808 s, 778 w, 702 m, 666 w, 576 s, 516 m.

Synthesis of $[Ag_2(\mu_4\text{-hmt})(\mu_4\text{-ox})]$ (5): The procedure was the same as that for **1**, yield ca. 75 %. Anal. calcd for $C_8H_{12}Ag_2N_4O_4$ **5**: C 21.64, H 2.72, N 12.62 %; found: C 21.48, H 2.61, N 12.52 %; IR (KBr, cm^{-1}): $\tilde{\nu}$ = 3428 m, 2979 m, 2945 m, 2864 w, 1578 vs, 1448 m, 1356 w, 1298 s, 1235 s, 1008 vs, 815 s, 770 s, 685 s, 519 w, 471 w, 403 w.

Synthesis of $[Ag_3(\mu_4\text{-hmt})_2(H_2O)_2](SO_4)(HSO_4)\cdot H_2O$ (6): White Ag_2SO_4 solid (0.117 g, 0.5 mmol) was added to a dilute H_2SO_4 solution (10 mL) over 10 min. The pH of the solution was adjusted to ≈4.5 by addition of dilute NaOH solution, then a solution of hmt (0.140 g, 1.0 mmol) in MeCN (5 mL) was slowly added. The resulting colorless solution was stirred at 50 °C for 15 min and allowed to stand in air at room temperature for three weeks, yielding colorless crystals, yield ca. 55 % based on silver(I). Anal. calcd for $C_{12}H_{36}Ag_3N_8O_{10}S_2$ **6**: C 17.97, H 3.77, N 13.97 %; found: C 17.68, H 3.64, N 13.75 %; IR (KBr, cm^{-1}): $\tilde{\nu}$ = 3458 s, 3409 s, 2959 m, 2931 w, 2882 m, 1630 m, 1560 w, 1461 m, 1398 w, 1377 w, 1349 w, 1293 m, 1257 s, 1236 s, 1110 vs, 1011 vs, 871 w, 814 s, 688 m, 617 s, 505 w.

Synthesis of $[Ag_2(\mu_4\text{-hmt})(\mu_2\text{-}O_2CMe)](MeCO_2)\cdot 4.5H_2O$ (7): The procedure was the same as that for **1**, yield ca. 75 %. Anal. calcd for $C_{10}H_{27}Ag_2N_4O_{8.5}$ **7**: C 21.64, H 4.90, N 10.09 %; found: C 21.48, H 4.79, N 10.04 %; IR (KBr, cm^{-1}): $\tilde{\nu}$ = 3325 s br, 2938 m, 2875 m, 1672 m, 1574 vs, 1454 m, 1405 s, 1342 m, 1236 s, 1046 w, 920 w, 814 m, 688 m, 646 m, 625 w, 512 w.

Synthesis of $[Ag_2(\mu_4\text{-hmt})(\mu_3\text{-maleate})]\cdot 5H_2O$ (8): The procedure was the same as that for **1**, ca. 82 % yield. Anal. calcd for $C_{10}H_{24}Ag_2N_4O_9$ **8**: C 21.45, H 4.32, N 10.00 %; found: C 21.28, H 4.19, N 9.84 %; IR (KBr, cm^{-1}): $\tilde{\nu}$ =

Table 1. Crystallographic data for compounds **1**–**11**.

	$[Ag_2(hmt)(NO_2)_2]$ (**1**)	$[Ag_2(hmt)(SO_4)(H_2O)]\cdot 4H_2O$ (**2**)	$[Ag(hmt)(NO_2)]$ (**3**)	$[Ag_2(hmt)_2](S_2O_6)\cdot 2H_2O$ (**4**)	$[Ag_2(hmt)(ox)]$ (**5**)	$[Ag_3(hmt)_2(H_2O)_2](SO_4)(HSO_4)\cdot 2H_2O$ (**6**)
empirical formula	$C_6H_{12}N_6O_4Ag_2$	$C_6H_{22}N_4O_9SAg_2$	$C_6H_{12}N_5O_2Ag$	$C_{12}H_{28}N_8O_8S_2Ag_2$	$C_8H_{12}Ag_2N_4O_4$	$C_{12}H_{33}N_8O_{12}S_2Ag_3$
M_r	447.96	542.08	294.08	692.28	443.96	869.19
crystal system	orthorhombic	monoclinic	orthorhombic	orthorhombic	monoclinic	orthorhombic
space group	*Pmma* (No. 51)	*Cc* (No. 9)	*Pnma* (No. 62)	*Pbca* (No. 60)	*P2/c* (No. 13)	*Pnnm* (No. 58)
a [Å]	12.882(6)	6.362(6)	12.951(5)	12.141(5)	6.383(2)	10.011(4)
b [Å]	6.2920(10)	18.81(1)	6.583(3)	11.140(2)	6.816(2)	19.369(7)
c [Å]	6.945(4)	12.552(4)	10.449(5)	15.765(9)	12.414(5)	6.4140(10)
β [°]	90	91.64(6)	90	90	92.95	90
V [Å^3]	562.9(4)	1502(2)	890.8(7)	2132.2(15)	539.4(3)	1243.7(7)
Z	2	2	4	8	2	2
ρ_{calcd} [g cm^{-3}]	2.643	2.398	2.193	2.157	2.734	2.321
μ [mm^{-1}]	3.498	2.798	2.245	2.093	3.644	2.581
obs. refl. criterion	$I > 2\sigma(I)$	$I > 2\sigma(I)$	$I > 2\sigma(I)$	$I > 2\sigma(I)$	$I > 2\sigma(I)$	$I > 2\sigma(I)$
$R1$, $wR2$[a, b]	0.0289, 0.0746	0.0259, 0.0663	0.0488, 0.1241	0.0485, 0.1377	0.0467, 0.1317	0.0386, 0.1031

[a] $R1 = \Sigma||F_o| - |F_c||/\Sigma|F_o|$. [b] $wR2 = [\Sigma w(F_o^2 - F_c^2)^2/\Sigma w(F_o^2)^2]^{1/2}$; weighting: $w = 1/[\sigma^2(F_o)^2 + (aP)^2 + bP]$, where $P = (F_o^2 + 2F_c^2)/3$.

	$[Ag_2(hmt)(O_2CMe)](MeCO_2)\cdot 4.5H_2O$ (**7**)	$[Ag_2(hmt)(maleate)]\cdot 5H_2O$ (**8**)	$[Ag_3(hmt)(O_2CPh)_3]$ (**9**)	$[Ag_4(hmt)_3(H_2O)](SO_4)(NO_3)_2\cdot 3H_2O$ (**10**)	$[Ag_{12}(hmt)_6(HPO_4)(H_2PO_4)_{10}(H_2O)](H_3PO_4)\cdot 10.5H_2O$ (**11**)
empirical formula	$C_{10}H_{27}N_4O_{8.5}Ag_2$	$C_{10}H_{24}N_4O_9Ag_2$	$C_{27}H_{27}Ag_3N_4O_6$	$C_{18}H_{44}N_{14}O_{14}SAg_4$	$C_{36}H_{119}Ag_{12}N_{24}O_{59.50}P_{12}$
M_r	555.10	560.07	827.14	1144.21	3506.63
crystal system	orthorhombic	monoclinic	triclinic	orthorhombic	monoclinic
space group	*Pbcn* (No. 60)	*C2/c* (No. 15)	$P\bar{1}$ (No. 2)	*Pnma* (No. 62)	$P2_1$ (No. 4)
a [Å]	22.7015(3)	12.587(7)	6.439(2)	29.402(13)	10.310(2)
b [Å]	12.1200(2)	22.311(10)	15.490(5)	6.543(2)	22.950(5)
c [Å]	12.9889(2)	13.063(7)	15.758(8)	16.849(9)	20.002(4)
α [°]	90	90	117.630(10)	90	90
β [°]	90	103.30(2)	90.930(10)	90	90.49(3)
γ [°]	90	90	94.370(10)	90	90
V [Å^3]	3573.79(9)	3570(3)	1386.1(9)	3241(2)	4732.6(17)
Z	8	8	2	4	2
ρ_{calcd} [g cm^{-3}]	2.164	2.084	1.982	2.345	2.461
μ [mm^{-1}]	2.251	2.246	2.147	2.534	2.744
obs. refl. criterion	$I > 2\sigma(I)$	$I > 2\sigma(I)$	$I > 2\sigma(I)$	$I > 2\sigma(I)$	$I > 2\sigma(I)$
$R1$, $wR2$[a, b]	0.0553, 0.1664	0.0475, 0.1192	0.0564, 0.1303	0.0531, 0.1371	0.0463, 0.1098

[a] $R1 = \Sigma||F_o| - |F_c||/\Sigma|F_o|$. [b] $wR2 = [\Sigma w(F_o^2 - F_c^2)^2/\Sigma w(F_o^2)^2]^{1/2}$; weighting: $w = 1/[\sigma^2(F_o)^2 + (aP)^2 + bP]$, where $P = (F_o^2 + 2F_c^2)/3$.

3325 s br, 2938 m, 2875 m, 1672 m, 1574 vs, 1454 m, 1405 s, 1342 m, 1236 s, 1046 w, 920 w, 814 m, 688 m, 646 m, 625 w, 512 w.

Synthesis of $[Ag_3(\mu_4\text{-hmt})(\mu_2\text{-}O_2CPh)_3]$ (9): The procedure was the same as that for **1**, yield ca. 86 %. Anal. calcd for $C_{27}H_{27}Ag_3N_4O_6$ **9**: C 39.21, H 3.29, N 6.77 %; found: C 39.16, H 3.22, N 6.72 %; IR (KBr, cm^{-1}): $\tilde{\nu} = 3057$ w, 2966 w, 2931 w, 1595 s, 1553 vs, 1453 w, 1391 s, 1229 s, 1173 w, 1068 w, 1004 vs, 835 w, 814 m, 709 s, 681 s, 512 w, 428 w.

Synthesis of $[Ag_4(\mu_4\text{-hmt})_3(H_2O)](SO_4)(NO_3)_2\cdot 3H_2O$ (10): An aqueous solution (5 mL) of hmt (0.140 g, 1.0 mmol) was added dropwise to a stirred MeCN/H_2O suspension (5 mL) of Ag_2SO_4 (0.156 g, 0.5 mmol) at 50 °C for 15 min. The solution was adjusted to pH ≈ 4.5 by addition of dilute HNO_3 solution. The resulting colorless solution was allowed to stand in air at room temperature for two weeks, yielding colorless crystals (ca. 90 % yield). Anal. calcd for $C_{18}H_{44}Ag_4N_{14}O_{14}S$ **10**: C 18.90, H 3.88, N 17.14 %; found: C 18.78, H 3.68, N 17.02 %; IR (KBr, cm^{-1}): $\tilde{\nu} = 3440$ m br, 2921 w, 1578 m, 1460 m, 1381 s, 1237 s, 1091 s, 1004 vs, 811 s, 688 s, 605 m, 506 m, 377 w.

Synthesis of $[Ag_{12}(\mu_4\text{-hmt})_6(\mu_3\text{-}HPO_4)(\mu_2\text{-}H_2PO_4)_3(H_2PO_4)_7(H_2O)](H_3PO_4)\cdot 10.5H_2O$ (11): Yellowish Ag_3PO_4 solid (0.5 mmol) was added to a dilute H_3PO_4 solution (15 mL) in 20 min. The solution was adjusted to pH ≈ 4.5 by addition of dilute NaOH solution, then a solution of hmt (0.280 g, 2.0 mmol) in MeCN (5 mL) was slowly added. The resulting colorless solution was stirred at 50 °C for 15 min and allowed to stand in air at room temperature for three weeks, yielding colorless crystals [ca. 55 % yield based on silver(I)]. Calc. for $C_{36}H_{119}Ag_{12}N_{24}O_{59.5}P_{12}$ **11**: C 12.33, H 3.42, N 9.59 %; found: C 12.19, H 3.34, N 9.55 %; IR (KBr, cm^{-1}): $\tilde{\nu} = 3451$ m br, 3388 m, 2952 m, 2875 m, 1651 m, 1560 m, 1461 m, 1370 w, 1300 w, 1264 m, 1236 s, 1075 m, 1011 vs, 934 m, 814 s, 688 m, 674 m, 540 m, 512 w.

X-ray crystallography: Diffraction intensities for the eleven complexes were collected at 21 °C on a Siemens R3m diffractometer using the ω-scan technique. Lorentz polarization and absorption corrections were applied.[23] The structures were solved by direct methods and refined with the full-matrix least-squares technique by means of the SHELXS-97 and SHELXL-97 programs, respectively.[24, 25] Anisotropic thermal parameters were assigned to all non-hydrogen atoms except those in **10**, in which some non-hydrogen atoms are refined anisotropically. The organic hydrogen atoms were generated geometrically (C–H = 0.96 Å); the aquo hydrogen atoms were located from difference maps and refined with isotropic temperature factors. Analytical expressions of neutral-atom scattering factors were employed, and anomalous dispersion corrections were incorporated.[26] The absolute structures for **3** and **11** were determined with Flack parameters of −0.03(4) and 0.09(4), respectively.[27] The crystallographic data for **1**–**11** are listed in Table 1. Drawings were produced with SHELXTL.[28] Crystallographic data (excluding structure factors) for the structures reported in this paper have been deposited with the Cambridge Crystallographic Data Centre as supplementary publications nos. CCDC-116813 to 116814 and CCDC-138324 to 138332. Copies of the data can be obtained free of charge on application to CCDC, 12 Union Road, Cambridge CB2 1EZ, UK (fax: (+44) 1223-336-033; e-mail: deposit@ccdc.cam.ac.uk).

Acknowledgements

This work was supported by the National Natural Science Foundation of China (No. 29625102, 29971033). We are indebted to the Chemistry Department of The Chinese University of Hong Kong for donation of the diffractometer.

[1] a) R. Robson, B. F. Abrahams, S. R. Batten, R. W. Gable, B. F. Hoskins, J. Lieu, *Supramolecular Architecture*, ACS, Washington, DC, **1992**, p. 256; b) J. M. Lehn, *Supramolecular Chemistry*, VCH, Weinheim, **1995**, ch. 9; c) S. R. Batten, R. Robson, *Angew. Chem.* **1998**, *110*, 1558; *Angew. Chem. Int. Ed.* **1998**, *37*, 1460; d) O. M. Yaghi, H. Li, C. Davis, D. Richardson, T. L. Groy, *Acc. Chem. Res.* **1998**, *31*, 474; e) M. Munakata, L. Wu, T. Kuroda-Sowa, *Adv. Inorg. Chem.* **1999**, *46*, 173; f) A. J. Blake, N. R. Champness, P. Hubberstey, W.-S. Li, M. A. Withersby, M. Schröder, *Coord. Chem. Rev.* **1999**, *183*, 117; g) P. J. Hagrman, D. Hagrman, J. Zubieta, *Angew. Chem.* **1999**, *111*, 2798; *Angew. Chem. Int. Ed.* **1999**, *38*, 2638.

[2] C. B. Aakeröy, K. R. Seddon, *Chem. Soc. Rev.* **1993**, 397.

[3] a) T. L. Hennigar, D. C. MacQuarrie, P. Losier, R. D. Rogers, M. J. Zaworotko, *Angew. Chem.* **1997**, *109*, 1044; *Angew. Chem. Int. Ed. Engl.* **1997**, *36*, 972; b) H. Gudbjartson, K. Biradha, K. M. Poirier, M. J. Zaworotko, *J. Am. Chem. Soc.* **1999**, *121*, 2599.

[4] M.-L. Tong, B.-H. Ye, X.-M. Chen, S. W. Ng, *Inorg. Chem.* **1998**, *37*, 2645.

[5] a) M.-L. Tong, X.-M. Chen, B.-H. Ye, S. W. Ng, *Inorg. Chem.* **1998**, *37*, 5168; b) L. Carlucci, G. Ciani, D. M. Proserpio, A. Sironi, *Angew. Chem.* **1995**, *107*, 2037; *Angew. Chem. Int. Ed. Engl.* **1995**, *34*, 1895.

[6] G. R. Desiraju, *Angew. Chem.* **1995**, *107*, 2541; *Angew. Chem. Int. Ed. Engl.* **1995**, *34*, 2311.

[7] O. Ermer, *J. Am. Chem. Soc.* **1988**, *110*, 3747.

[8] A. Michelet, B. Voissat, P. Khodadad, N. Rodier, *Acta Crystallogr. B* **1981**, *37*, 2171.

[9] a) T. C. W. Mak, *Inorg. Chim. Acta* **1984**, *84*, 19; b) T. C. W. Mak, *Jiegou Huaxue* (*Chin. J. Struct. Chem.*) **1985**, *4*, 16.

[10] L. Carlucci, G. Ciani, D. M. Proserpio, A. Sironi, *J. Am. Chem. Soc.* **1995**, *117*, 12861.

[11] L. Carlucci, G. Ciani, D. W. V. Gudenberg, D. M. Proserpio, A. Sironi, *Chem. Commun.* **1997**, 631.

[12] M. Bertelli, L. Carlucci, G. Ciani, D. M. Proserpio, A. Sironi, *J. Mater. Chem.* **1997**, *7*, 1271.

[13] L. Carlucci, G. Ciani, D. M. Proserpio, A. Sironi, *Inorg. Chem.* **1997**, *36*, 1736.

[14] M.-L. Tong, S.-L. Zheng, X.-M. Chen, *Chem. Commun.* **1999**, 561.

[15] a) R. L. Griffith, *J. Chem. Phys.* **1943**, *11*, 499; b) D. Yu. Naumov, A. V. Virovets, N. V. Podberezskaya, E. V. Boldyreva, *Acta Crystallogr. C* **1995**, *51*, 60; c) M. Julve, J. Faus, M. Verdaguer, A. Gleizes, *J. Am. Chem. Soc.* **1984**, *106*, 8306; d) S. Decurtins, H. W. Schmalle, P. Schneuwly, J. Ensling, P. Gütlich, *J. Am. Chem. Soc.* **1994**, *116*, 9521; e) G. De Munno, M. Julve, F. Nicolo, F. Lloret, J. Faus, R. Ruiz, E. Sinn, *Angew. Chem.* **1993**, *105*, 588; *Angew. Chem. Int. Ed. Engl.* **1993**, *32*, 613; f) A. Bino, F. A. Cotton, Z. Dori, *J. Am. Chem. Soc.* **1978**, *100*, 5252; g) R. Kaziro, T. W. Hambley, R. A. Binstead, J. K. Beattie, *Inorg. Chim. Acta* **1989**, *164*, 85; h) V. Masters, L. R. Gahan, C. H. L. Kennard, *Acta Crystallogr. C* **1997**, *53*, 1576; i) S. O. Dunham, R. D. Larsen, E. H. Abbott, *Inorg. Chem.* **1991**, *30*, 4328; j) Q. Chen, S. Liu, J. Zubieta, *Angew. Chem.* **1988**, *100*, 1792; *Angew. Chem. Int. Ed. Engl.* **1988**, *27*, 1724.

[16] Y.-X. Tong, X.-M. Chen, S. W. Ng, *Polyhedron* **1997**, *16*, 3363.

[17] M. Jansen, *Angew. Chem.* **1987**, *99*, 1136; *Angew. Chem. Int. Ed. Engl.* **1987**, *26*, 1098.

[18] a) B. Lippert, D. Neugebauer, *Inorg. Chem.* **1982**, *21*, 451; b) R. Villanneau, A. Proust, F. Robert, P. Gouzerh, *Chem. Commun.* **1998**, 1491.

[19] a) M. Fujita, Y. J. Kwon, S. W. Ashizu, K. Ogura, *J. Am. Chem. Soc.* **1994**, *116*, 1151; b) C. Janiak, *Angew. Chem.* **1997**, *109*, 1499; *Angew. Chem. Int. Ed. Engl.* **1997**, *36*, 1431; c) O. M. Yaghi, H. Li, *J. Am. Chem. Soc.* **1996**, *118*, 295.

[20] D. W. Breck in *Zeolite Molecular Sieves, Structure, Chemistry, and Use*, John Wiley, New York, **1974**.

[21] a) T. M. Reineke, M. Eddaoudi, M. Fehr, D. Kelley, O. M. Yaghi, *J. Am. Chem. Soc.* **1999**, *121*, 1651; b) T. M. Reineke, M. Eddaoudi, M. Fehr, D. Kelley, O. M. Yaghi, *Angew. Chem.* **1999**, *111*, 2712; *Angew. Chem. Int. Ed.* **1999**, *38*, 2590.

[22] T. C. W. Mak, W.-H. Yip, C. H. L. Kennard, G. Smith, E. J. O'Reilly, *Aust. J. Chem.* **1986**, *39*, 541.

[23] A. C. T. North, D. C. Phillips, F. S. Mathews, *Acta Crystallogr. A* **1968**, *24*, 351.

[24] G. M. Sheldrick, *SHELXS-97, Program for X-Ray Crystal Structure Solution*, Göttingen University (Germany), **1997**.

[25] G. M. Sheldrick, *SHELXL-97, Program for X-Ray Crystal Structure Refinement*, Göttingen University (Germany), **1997**.

[26] *International Tables for X-Ray Crystallography*, *Vol. C*, Tables 4.2.6.8 and 6.1.1.4., Kluwer, Dordrecht, **1992**.

[27] H. D. Flack, *Acta Crystallogr. A* **1983**, *39*, 876.

[28] G. M. Sheldrick, *SHELXTL* Version 5, Siemens Industrial Automation, Madison, Wisconsin (USA), **1995**.

Received: January 3, 2000
Revised version: April 14, 2000 [F2220]

  0947-6539/00/0620-3738 $ 17.50+.50/0